Close-packed structures and phase diagram of soft spheres in cylindrical pores

Kenichiro Koga[a] and Hideki Tanaka
Department of Chemistry, Faculty of Science, Okayama University, 3-1-1 Tsushima-naka, Okayama 700-8530, Japan

It is shown for a model system consisting of spherical particles confined in cylindrical pores that the first ten close-packed phases are in one-to-one correspondence with the first ten ways of folding a *triangular lattice*, each being characterized by a roll-up vector like the single-walled carbon nanotube. Phase diagrams in pressure-diameter and temperature-diameter planes are obtained by inherent-structure calculation and molecular dynamics simulation. The phase boundaries dividing two adjacent phases are infinitely sharp in the low-temperature limit but are blurred as temperature is increased. Existence of such phase boundaries explains rich, diameter-sensitive phase behavior unique for cylindrically confined systems. © *2006 American Institute of Physics.*
[DOI: 10.1063/1.2172592]

Packing problems in various dimensions are not only of great interest in mathematics and basic science but also are highly relevant to material engineering as crystal structure is key in determining material properties. Computational studies have proved essential to make progress in this subject too.[1–3] Pickett *et al.*[3] showed that close-packed hard spheres in a cylinder take several chiral and achiral structures as the cylinder diameter is varied. Hodak and Girifalco[4] then demonstrated that a model system of C_{60} molecules in carbon nanotubes (soft spheres in a cylinder) also exhibits various ordered phases including those found for the hard-sphere system. Subsequently experimental evidences were reported that C_{60} molecules form some of the predicted structures when packed in boron nitride nanotubes[5] and carbon nanotubes.[6]

These results for different systems imply generic phase behavior of spherical particles in cylindrical cavities; however, our knowledge on possible phases is yet fragmentary, no explanation is given as to why in such order these chiral and achiral structures appear, and phase transformations among them is little explored. Main purposes of this communication are first to show all the possible solid phases of soft spheres in a cylindrical pore whose effective dimensionless diameter (defined below) is less than 3, and then to predict and account for the phase behavior of cylindrically confined materials under various conditions by obtaining phase diagrams in the pressure-diameter and temperature-diameter planes.

We study a system consisting of Lennard-Jones (LJ) particles confined in a cylindrical tube. The LJ size and energy parameters are taken to be those for argon: $\sigma = 3.4$ Å and $\epsilon/k = 120$ K with k being Boltzmann's constant. Each LJ particle interacts with the inner surface of the tube by a potential function only of the distance of the particle from the tube axis: The function is of the form obtained by integrating an LJ 12-6 potential over the cylindrical surface, where the LJ parameters are those for the argon-carbon interaction: $(\sigma + \sigma_C)/2$ and $\sqrt{\epsilon \epsilon_C}$ with $\sigma_C = 3.4$ Å and $\epsilon_C/k = 28.0$ K[9] and the area density of the surface is equal to that of carbon atoms in the single-walled carbon nanotube (SWCN).[7,8] The periodic boundary condition in the axial direction is not employed for the present system because it imposes translational periodicity on nonperiodic chiral solid phases; instead, smooth walls are placed at both ends of the tubule. The number N of particles is taken to be 180 for most of the calculations. Then the tubule length l ranges from 120 Å for the diameter d of the (16, 0) SWCN to 360 Å for d of the (12, 0) SWCN. It is confirmed that larger systems ($N = 270, 360$) exhibit essentially the same phase behavior at arbitrary chosen conditions.

The first crucial step in the present study is to identify, within a prescribed range of d, all the possible chiral and achiral phases of the confined particles. In this step a conjecture on close-packed structures in cylindrical geometry is presented and stability and structural properties of the proposed structures at 0 K are examined by the inherent-structure calculation.[10] Whether or not these structures are formed spontaneously from liquidlike structures are checked by molecular dynamics (MD) simulation. The second step, and our main goal, is to construct phase diagrams allowing us to predict the phase behavior in the pressure-temperature-diameter space. The phase diagram in the pressure-diameter plane at 0 K is accurately given by the inherent-structure calculations while a phase diagram in the temperature-diameter plane is obtained from series of the MD simulations along isothermal-isobaric paths. In each calculation, we fix the tube diameter d, the pressure-tensor component P_A parallel to the axis of tubule, and temperature T (in the inherent-structure calculation $T = 0$ K). The isobaric-isothermal ensemble is achieved by Nosé-Andersen's method[11] with modification to control P_A instead of bulk pressure. The equilibration at each state point is assured by no steady drift in thermodynamic properties and by reproducibility of these

---
[a] Electronic mail: koga@cc.okayama-u.ac.jp

properties in independent calculations. Thermodynamic states we examine here cover the following ranges of the three variables: $0.1 \text{ MPa} \leq P_A \leq 1 \text{ GPa}$; $0 \text{ K} \leq T \leq 120 \text{ K}$; and $d < 13.5 \text{ Å}$. The diameter range includes diameters of the "zigzag" $(n, 0)$ SWCNs with $n \leq 17$. For comparisons with other analogous systems (such as the hard spheres in a hard cylinder and C_{60} in the nanotube), it is convenient to express the diameter in terms of an *effective* dimensionless form: $D = (d - \sigma_C)/\sigma$, where σ and σ_C are the LJ size parameters for argon and carbon. The diameter range is then $D \leq 2.97$. The simulation time at each state is typically 200 ns and if necessary extended to 1 μs.

It is known that hard spheres closely packed in a cylindrical cavity take six distinct phases in a range of $1 \leq D \leq 1 + 2/\sqrt{3} \sim 2.15$ (here D is the hard-cylinder diameter in units of the hard-sphere diameter) and, although the packing fraction itself is continuous, its derivative with respect to D is discontinuous at analytically given phase boundaries.[3] Now we wish to examine the corresponding phase behavior for LJ particles (soft spheres) confined in a cylindrical tube. But first of all we must ask: Do we *know* all the possible close-packed phases with respect to a certain range of D? As the recent studies on C_{60} showed,[4–6] our preliminary MD simulations indicate that the closely packed soft spheres take various distinct structures, including those found for hard spheres, at discrete values of the tube diameter. Furthermore, unrolling any of these structures to a plane gives rise to a configuration very close to the regular triangular lattice—the close-packed configuration of spheres in two dimensions.[4] One can then anticipate reversely: A set of distinct ways of folding the triangular lattice into a quasi-one-dimensional (Q1D) structure is in one-to-one correspondence with a set of possible close-packed phases in a tube of $D \leq D_c$ where D_c is an upper limit of the diameter. We show below that this conjecture is supported for $D_c \simeq 3$. Each way of folding is specified by (n, m), a vector connecting two equivalent sites in the triangular lattice, in the same way as is done for the carbon nanotube.[8] Any (n, m) structure is achiral if $n = m$ or $m = 0$ and is chiral otherwise, again as it is so for the carbon nanotube. Furthermore, a chiral structure $(n > m > 0)$ is described by a single helix if $m = 1$ and double helices if $m = 2$. Figure 1 illustrates three roll-up vectors on the triangular lattices and the corresponding folded structures. See the figure caption for how to fold the triangular lattice into the 3d structures.

Table I lists the ten thinnest folded structures. Exact positions of particles in each folded structure are determined. In cases of chiral structures, the position of the ith particle in a helix is described by cylindrical coordinates $(r, i\Delta\phi, i\Delta z)$, where the second and third components are to be shifted by certain amounts for the other helices in a folded structure.[3] Folded structures can be counted up further but the empty space along the axis grows with r and eventually becomes large enough to accommodate additional spheres, that is, they cannot be close-packed structures. In fact we will see that the $(5, 0)$ structure is more stable when its voids along the axis is closely packed with spheres than when it is empty.

The inherent-structure analysis below shows that the ten folded structures are indeed possible phases which we shall
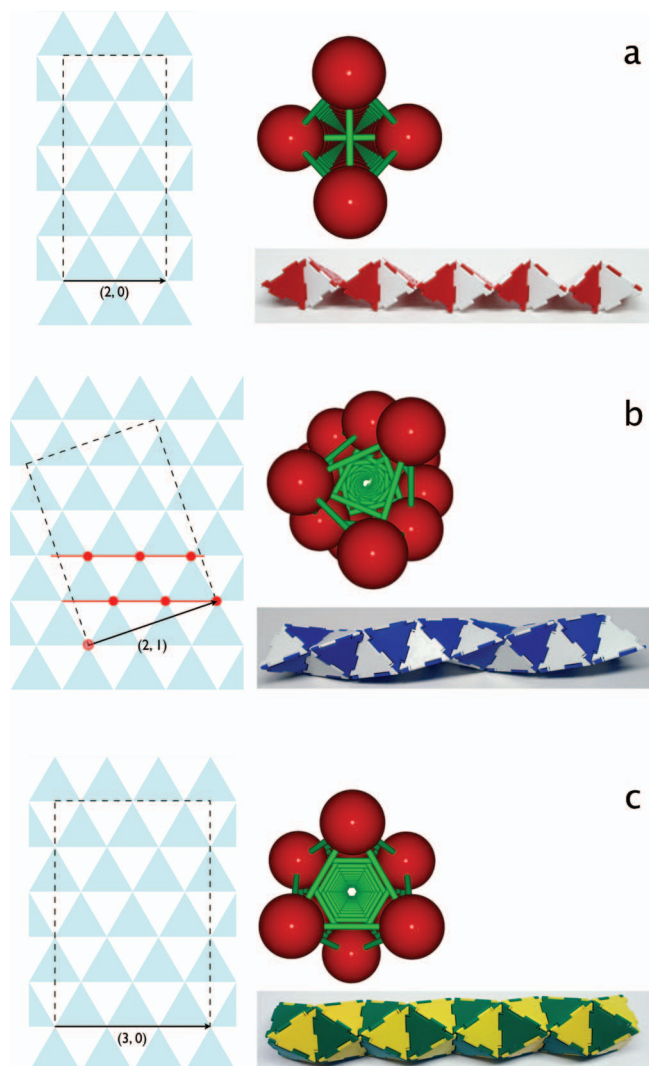

FIG. 1. (Color) Roll-up vectors (2, 0), (2, 1), and (3, 0) on triangular lattices and photographs of the resulting folded structures (side view). Computer graphics (top view) show the structures of "argon" in nanotubes obtained by simulation. Transformation from a triangular lattice sheet to each 3d structure can be done in the same manner as *origami*, the Japanese art of folding paper: Fold the sheet (without bending each side of triangles) matching any two vertices corresponding to the head and tail of the roll-up vector.

refer to as I, II,…,X. First, one prepares configurations of folded structures in the tube and performs the steepest-descent calculation to map the initial structures to inherent structures at fixed P_A and diameter d. Then one finds that the inherent structures are essentially identical to the ideally folded structures if d is fixed to an appropriate value for each folded structure. Second, one successively performs the steepest-descent calculations by changing the tube diameter 0.01 or 0.02 Å. Then one finds a finite range of d for each inherent structure within which the positions of atoms vary smoothly with d while keeping its basic structure characterized by the roll-up vector. A quantity $U + P_A V$, where U is the potential energy and V is the volume of the system, of each inherent structure under constant P_A, when plotted against d, is a smooth curve in each range of d and two curves in neighboring ranges of d intersect in one point [see Fig. 2(a)]. This indicates each curve corresponds to one *phase* and the point of intersection is the phase boundary between two

TABLE I. Ten thinnest close-packed structures of spheres in cylinders and the corresponding phases of argon in the carbon nanotube. The term "single" and "double" indicate chiral structures described by single and double helices, respectively. The phase boundary points at 1 MPa for the inherent structures are given by the effective diameter D_{max} and the nanotube diameter d_{max}.

Structure	D	Chirality	Phase	D_{max} $(d_{max}/\text{Å})$
(1, 1)	$1+\sqrt{3}/2$		I	2.00 (10.21)
(2, 0)	2		II	2.04 (10.34)
(2, 1)	$1+3\sqrt{3}/5$	chiral, single	III	2.24 (11.00)
(3, 0)	$1+2/\sqrt{3}$		IV	2.31 (11.24)
(2, 2)	$1+\sqrt{6}/2$		V	2.43 (11.68)
(3, 1)	$2.2905\cdots$	chiral, single	VI	2.53 (12.00)
(4, 0)	$1+\sqrt{2}$		VII	2.64 (12.36)
(3, 2)	$2.4863\cdots$	chiral, double	VIII	2.73 (12.67)
(4, 1)	$2.5712\cdots$	chiral, single	IX	2.93 (13.36)
(5, 0)	$1+1/\sin(\pi/5)$		X	

phases at given P_A.[12] Note here that the tenth phase X is the filled (5, 0) structure which has additional spheres packed inside voids of the original (5, 0) structure; this is because the free energy $U+P_A V$ at 0 K of the filled structure is lower than that of the original one (and as we will see the former is spontaneously formed at finite temperatures in MD simulations). Also note that there is a change of concavity of the free-energy curve of phase I [Fig. 2(a)]; but in this case it is not the violation of thermodynamic stability conditions. In
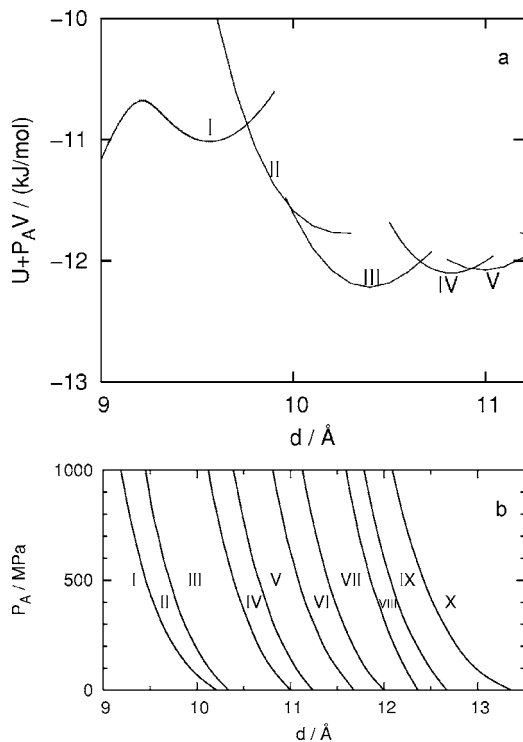

FIG. 2. (a) Free-energy curves $U+P_A V$ for first five phases at 0 K and $P_A = 200$ MPa and (b) the phase diagram in the P_A-d plane at 0 K. The abscissa d is the tube diameter and the ordinate P_A is the axial pressure. In (a) first five curves and four intersections are shown to illustrate how the phase boundaries are determined at 0 K; in (b) the diagram includes first ten thinnest close-packed phases, each corresponding to a folded structure given in Table I.

this way, one finds nine points of d that divides ten phases at fixed P_A and, after doing the same calculations as changing P_A, one obtains nine curves in the P_A-d plane at $T=0$. In Table I are listed the nine diameters of the phase boundaries at 1 MPa. In Fig. 2(b) is shown the phase diagram in the P_A-d plane including the nine phase boundaries. The slope $(\partial P_A/\partial d)_T$ of each phase boundary is negative and it gets steeper as P_A increases. The phase diagram indicates that two or three phase transitions occurs as P_A is increased up to 1 GPa. At $d=10.3$ Å, for instance, structural transformations take place from the (2, 0) achiral form (phase II) to the (2, 1) chiral structure (phase III) at 20 MPa, and then to the (3, 0) achiral structure (phase IV) at 650 MPa. Structure of each phase is unambiguously characterized by the roll-up vector (m, n). Phase I is, however, an exception: Within its range of d the structure changes from a linear chain to a zigzag planner to a single helix as observed in the hard-sphere system.[3] The first form is just a limiting case of the second, but the third has different chirality. However, the change occurs smoothly and all the thermodynamic properties are continuous in its range of d. The roll-up vector (1, 1) is assigned to phase I since it characterizes the zigzag planner form.

The MD simulations starting from random configurations of the particles in the tube demonstrate formation of the ordered configurations as conjectured. Fluid states equilibrated at high T and low P_A are transformed, either in low-T or high-P_A conditions, to solid states whose structures are identical to the first ten folded structures at diameters in the respective ranges shown in Table I and Fig. 2(a). The tenth solid phase has indeed the filled (5,0) structure. (If d is increased further one finds phases XI, XII,… of multilayer structures, inner structure of which develops with d just like the single-layer close-packed structure does.) We thus conclude that a set of the first ten ways of folding the triangular lattice is in one-to-one correspondence with a set of first ten close-packed phases of the cylindrically confined spherical particles.

One-dimensional systems at finite temperature may exhibit unusual phase behavior that a disordered state is *continuously* transformed to an ordered state.[13] The present system is not an exception: The MD simulations show, for example, that at the diameter of the (13, 0) carbon nanotube a liquidlike state is *gradually* transformed to the chiral (2, 1) solid in a range of T under 200 MPa, but this does *not* mean that the tube diameter is too narrow to make abrupt freezing possible. In fact, as we will see in a moment, freezing behavior (sharpness of freezing) of the cylindrically confined particles is so sensitive to the diameter d that it changes qualitatively if d is varied by 0.5 Å.

Figure 3 shows a phase diagram in the isobaric T-d plane at $P_A = 200$ MPa. Nine phase boundaries are nearly parallel to each other, have large positive slope, and extend from the nine points at $T=0$ K [corresponding to nine points at 200 MPa in Fig. 2(b)]. Each boundary is obtained from the MD simulations alone (i.e., without performing additional free-energy calculations) in the following way: (1) Perform sets of the MD simulations along isothermal paths in the T-d plane, where increment of d is taken to be as small as 0.02 Å. Thermodynamic equilibrium at each point of d is
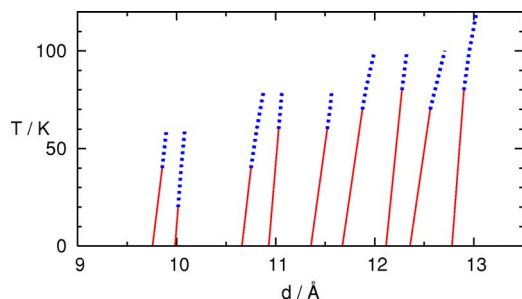
FIG. 3. (Color online) Phase diagram of argon in the *T-d* plane at 200 MPa. The solid lines indicate the phase boundaries at which abrupt transitions occur while the dotted lines are extension of the phase boundaries in the single-phase region, which are given by trajectories of inflection points of the isothermal-isobaric *V-d* curve.

checked by independent runs starting from opposite ends of a range of d. The obtained d-V isotherms look similar to P-V isotherms above and below the critical temperature in a bulk system. (2) Identify temperature T_c above which the d-V isotherms are continuous. For each such isotherm locate an inflection point d_i where a magnitude of the slope $(\partial V/\partial d)_T$ is maximum. (3) Series of the inflection points $d_i(T > T_c)$ and the point $d_i(T = 0)$ of the corresponding phase boundary at 0 K can be fit to a near linear function of T. Of each curve in Fig. 3 the segment below T_c (solid curves) is a phase boundary where first-order-like transitions are observed; the other segment above T_c (dashed curves) indicates a series of the inflection points around which occurs a continuous phase change. The dashed segments in the figure may be extended to higher T. The T_c is relatively low ($T_c < 50$ K) for boundaries in small d region and high ($T_c > 50$ K) for those in large d region. The II-III phase boundary has the lowest T_c ~ 20 K and the VII-VIII and IX-X phase boundaries have the highest $T_c \sim 80$ K (which is close to the triple point temperature of bulk argon) among the nine boundaries. It is clear from the phase diagram that if d is varied at low T, though it is impractical in experiments, then the system exhibits nine abrupt phase changes in the range of about 4 Å; if T is varied at fixed d, as in common experiments, on the other hand, then it exhibits at most a single abrupt change and is more likely to undergo gradual phase change. This is because the sum of the ranges where the phase boundaries exist is 30% of the whole d range (from 9.5 to 13.5 Å).

The MD simulations of a model system for argon in SWCNs show that the system exhibits abrupt and gradual phase changes below and above some temperature T_c. Simulations of water in the SWCNs also showed that phase change involving ordered ice nanotubes can be either discontinuous or continuous.[13,14] On the other hand, exactly solvable microscopic models[15,16] and phenomenological arguments[17] support that systems in less-than-two dimensions exhibit no phase transitions. Aside from rigorous discussions, it is anticipated that the real system too exhibits the same two types of phase behavior as found here, one of them

would be *observed* as a first-order phase transition within experimental accuracy. The solid structures, the phase boundaries, and the phase behavior reported here are expected to be robust for other analogous systems such as C_{60}, liquid metals, and other spherical particles confined in carbon nanotubes[18–26] and colloidal particles in cylindrical pores.

[1] T. C. Hales, xxx.lanl.gov/math.MG/9811071 (1998).
[2] A. Donev, I. Cisse, D. Sachs, E. A. Variano, F. H. Stillinger, R. Connelly, S. Torquato, and P. M. Chaikin, Science **303**, 990 (2004).
[3] G. T. Pickett, M. Gross, and H. Okuyama, Phys. Rev. Lett. **85**, 3652 (2000).
[4] M. Hodak and L. A. Girifalco, Phys. Rev. B **67**, 075419 (2003).
[5] W. Mickelson, S. Aloni, W.-Q. Han, J. Cumings, and A. Zettl, Science **300**, 467 (2003).
[6] A. N. Khlobystov, D. A. Britz, A. Ardavan, and G. A. Briggs, Phys. Rev. Lett. **92**, 245507 (2004).
[7] S. Iijima, Nature (London) **354**, 56 (1991).
[8] N. Hamada, S. Sawada, and A. Oshiyama, Phys. Rev. Lett. **68**, 1579 (1992).
[9] W. A. Steele, *Interaction of Gases with Solid Surfaces* (Pergamon, Oxford, 1974).
[10] F. H. Stillinger and T. A. Weber, Phys. Rev. A **25**, 978 (1982); Inherent structure means the structure any deviation from which increases the potential energy. To obtain the inherent structure at given P_A, steepest-descent calculation at fixed V with subsequent slight alteration to V (i. e., tubule length l) are repeated until the pressure converged to P_A within a prescribed precision.
[11] D. C. Rapaport, *The Art of Molecular Dynamics Simulations* (Cambridge University, Cambridge, 1997).
[12] For the system under fixed P_A at $T = 0$ K, a stable state is the one that minimizes $U + P_A V$ and two states can be equally stable only when they have the same minimal $U + P_A V$.
[13] K. Koga, G. T. Gao, H. Tanaka, and X. C. Zeng, Nature (London) **412**, 802 (2001).
[14] K. Koga, G. T. Gao, H. Tanaka, and X. C. Zeng, Physica A **314**, 462 (2002).
[15] C. Domb, Adv. Phys. **9**, 149 (1960).
[16] H. E. Stanley, *Introduction to Phase Transitions and Critical Phenomena* (Oxford University, New York, 1971), p. 116.
[17] L. D. Landau and E. M. Lifshitz, *Statistical Physics, Part I*, 3rd ed. (Butterworth-Heinemann, Oxford, 1980), p. 537.
[18] P. M. Ajayan and S. Iijima, Nature (London) **361**, 333 (1993).
[19] M. R. Pederson and J. Q. Broughton, Phys. Rev. Lett. **69**, 2689–2692 (1992).
[20] E. Dujardin, T. W. Ebbesen, H. Hiura, and K. Tanigaki, Science **265**, 1850 (1994).
[21] S. C. Tsang, Y. K. Chen, P. J. F. Harris, and M. L. H. Green, Nature (London) **372**, 159 (1994).
[22] D. Ugarte, A. Chatelain, and W. A. de Heer, Science **274**, 1897 (1996).
[23] C. H. Kiang, J. S. Choi, T. T. Tran, and A. D. Bacher, J. Phys. Chem. B **103**, 7449 (1999).
[24] R. S. Ruoff, D. C. Lorents, B. Chan, R. Malhotra, and S. Subramoney, Science **259**, 346 (1993).
[25] C. Guerret-Piecourt, Y. Le Bouar, A. Loiseau, and H. Pascard, Nature (London) **372**, 761 (1994).
[26] R. R. Meyer, J. Sloan, R. E. Dunin–Borkowski, A. I. Kirkland, M. C. Novotny, S. R. Bailey, J. L. Hutchison, and M. L. H. Green, Science **289**, 1324 (2000).